

Measuring anisotropic scattering in the cuprates

K. G. Sandeman¹ and A. J. Schofield²

¹*Low Temperature Physics Group, Cavendish Laboratory,
Madingley Road, Cambridge, CB3 0HE, United Kingdom.*

²*School of Physics and Astronomy, University of Birmingham,
Edgbaston, Birmingham B15 2TT, United Kingdom.*

(Dated: October 30, 2018)

A simple model of anisotropic scattering in a quasi two-dimensional metal is studied. Its simplicity allows an analytic calculation of transport properties using the Boltzmann equation and relaxation time approximation. We argue that the c -axis magnetoresistance provides the key test of this model of transport. We compare this model with experiments on overdoped Tl-2201 and find reasonable agreement using only weak scattering anisotropy. We argue that optimally doped Tl-2201 should show strong angular-dependent magnetoresistance within this model and would provide a robust way of determining the in-plane scattering anisotropy in the cuprates.

I. INTRODUCTION

The unusual transport properties in the normal state of the cuprates continue to attract widespread interest. Many aspects differ significantly from transport in conventional metals¹. The resistivity is linear in temperature² with scattering which is apparently electronic rather than electron-phonon in origin³. The Hall effect shows strong temperature dependence¹. On doping with zinc, both the resistivity and inverse Hall angle show a rather simple Matthiessen's rule⁴, suggestive of additive scattering mechanisms. However, their temperature dependences differ significantly. This has led to the suggestion that the resistivity and the inverse Hall angle are controlled by very different scattering rates (the so-called 'two-lifetime' behavior)⁵. This view seems to be confirmed by optical measurements⁶ which suggest two independent scattering rates in these materials. The magnetoresistance does not follow Kohler scaling behavior but appears also to be controlled by the Hall angle scattering rate⁷. Attempts to understand this behavior may be divided into three categories.

Anderson⁵ has argued that a non-Fermi liquid description must be invoked to understand transport in the cuprates. In Anderson's picture the electron decays into holons and spinons which separately control resistivity and magneto-transport respectively. A phenomenological transport equation was introduced by Coleman, Schofield and Tsvelik⁸ to capture a model of transport where the two lifetimes are controlled by independent fluids of particles.

A second approach argues that the magnetic field plays a special role in the transport process. In the model of Kotliar, Sengupta and Varma⁹ a singular skew scattering term is invoked. In the picture by Lee and Lee¹⁰ only recombined slave-fermion and slave-boson particles can interact with the true applied magnetic field. The slave particles themselves are insensitive to the true field because of the large fluctuations in the fictitious gauge field. In both of these scenarios the measured cyclotron frequency would appear to be temperature dependent—a

result at odds with current optical Hall experiments¹¹.

The third possibility—the 'anisotropic scattering' scenario—envisages a conventional metallic state characterized by an electron quasiparticle scattering rate which depends strongly on the particle momentum. This picture was first suggested by Cooper¹² and has been further elaborated upon by Stojković and Pines¹³, and also by Yakovenko and coworkers^{14,15}. Pines *et al.* argue that antiferromagnetic fluctuations in the normal state strongly scatter regions on the Fermi surface which are connected by the antiferromagnetic wave vector. Regions away from these 'hot-spots' are weakly scattered. However, Hlubina and Rice¹⁶ have claimed that the cold regions would tend to 'short-circuit' the hot spots, thereby leading to conventional transport at low temperatures. Ioffe and Millis¹⁷ have introduced a new variant on the anisotropic scattering picture which is partly motivated by the short-circuiting problem and also inspired by the direct measurements of electron lifetimes. They use angle-resolved photoemission data to argue that quasiparticles are very strongly scattered over most of the Fermi surface. The only long-lived quasiparticles are found at the zone diagonals, where they decay with a weak T^2 Fermi liquid form. This is known as the 'cold spot' model and has been used to understand a wide variety of experiments (see for example Van der Marel¹⁸ and Xiang and Hardy¹⁹).

In this paper we consider this third scenario of anisotropic scattering and treat a minimal model which we believe is illustrative of the strengths and weaknesses of this approach (similar in spirit to some treatments of the cuprate superconducting state²⁰). Whilst more sophisticated treatments exist, either with a specific relaxation mechanism^{13,21} or in the limit of extremely anisotropic in-plane scattering¹⁷, there are advantages to this model's simplicity. We can obtain analytic expressions for a wide range of transport properties over the full range of anisotropy. Our calculations illustrate the conclusions of Ioffe and Millis in the limit of strong anisotropy, but also allow us to see how this evolves from the more familiar isotropic metal. This is important as the approach to the isotropic limit may be more rele-

vant to experiments on overdoped materials where the two-lifetime behavior is less apparent. We also consider the transition to the intermediate and high field regimes of magnetoresistance within this picture, and non-linear effects at high electric field.

Perhaps the key discrepancy between the ‘cold-spot’ model and the transport properties of the cuprates is the in-plane orbital magnetoresistance. The model predicts a large magnetoresistance with a distinct temperature dependence in contrast with current experiments. This was noted in Ioffe and Millis’ original paper¹⁷ and is reproduced in passing here. It has been argued that proper inclusion of vertex corrections could account for this discrepancy^{22,23}. The most important new work in this paper is to consider the orbital magnetoresistance for currents moving along the c -axis. The c -axis conductivity in a quasi-two dimensional metal may be computed *without* vertex corrections²⁴ and so should be a robust feature of this scenario. We show how an in-plane magnetic field affects the c -axis conductivity and argue that this experimental geometry provides a key test of the model. Indeed experiments exist on Tl-2201²⁵ but only in the overdoped regime where the two lifetimes become less distinct. Nevertheless our complete solution of an anisotropic scattering model allows us to obtain a reasonable fit to the data provided we include both scattering anisotropy and bandstructure effects.

Our main conclusions are that within our model the in-plane magnetoresistance remains an outstanding problem if this model is to fit the experiment—not just from its magnitude and temperature dependence but from the scale at which deviations from the weak-field regime occur. While a proper treatment of vertex corrections may correct this for in-plane properties, the c -axis magnetoresistance is insensitive to these corrections and provides a robust test of the model. Experiments here have mainly been done on overdoped cuprates and our detailed fit to experiments are consistent with this model. High field c -axis measurements on optimally doped cuprates should be made to test unambiguously this transport phenomenology.

This paper is planned as follows. In section II we present our models of scattering and bandstructure which are the ingredients for the analytic calculation of transport properties. The results are to be found in Section III. These are displayed in the general case, and also in the limit of large scattering anisotropy. Both in-plane and out-of-plane magnetoresistivity are shown, and compared with experimental observations in section IV. Non-ohmic in-plane conductivity is also calculated. Conclusions are drawn in section V.

II. ANISOTROPIC TRANSPORT

Our main assumption in this work is to use a Boltzmann equation within the relaxation time approximation as a description of transport. We write the collision in-

tegral, $I[f]$, as $-\Gamma_{\mathbf{k}}[f(\mathbf{k}) - f^{(0)}(\mathbf{k})]$ and impose a phenomenological scattering rate, $\Gamma_{\mathbf{k}}$, which varies smoothly around the in-plane Fermi surface and has square symmetry.

We do not speculate on the underlying cause of the quasiparticle relaxation rate but, if this scattering were due to scattering from a soft bosonic mode at finite \mathbf{Q} (antiferromagnetic spin fluctuations for example), then the validity of the relaxation time approximation might be questionable²⁶. This is because such scattering would tend to equilibrate quasiparticles only between points on the Fermi surface connected by the spanning vector (\mathbf{Q}) of the mode. By contrast, the relaxation time approximation assumes that the quasiparticle is equilibrated uniformly around the Fermi surface. This will not affect our calculation of c -axis response if the bosonic mode is 2-dimensional, but it could change the in-plane physics. This is presumably the reason why vertex corrections could be important for in-plane transport. However, including this process correctly would tend to make the quasiparticle distribution even more anisotropic when driven out of equilibrium. As we will see, the anisotropy of the out-of-equilibrium distribution of quasiparticles is precisely what is probed by the in-plane magnetoresistance. Increasing this anisotropy is likely to increase further the in-plane magnetoresistance.

Within the relaxation time approximation we now introduce two forms of scattering rate to model the anisotropy.

A. The cold-spot model

Following Ioffe and Millis¹⁷, the angle-resolved photoemission results suggest that there are points on the Fermi surface where the electron is a fairly long-lived excitation: points where the Fermi surface intersects the Brillouin zone diagonal. Elsewhere on the Fermi surface, only broad features in energy are seen in the photoemission. Within a Fermi liquid picture one would then infer that electron-like quasiparticles are strongly scattered everywhere except for these special points. We can capture this by the following form for our scattering rate

$$\Gamma(k_{\parallel}, \theta, k_{\perp}) = \Gamma_f \cos^2 2\theta + \Gamma_s \sin^2 2\theta. \quad (1)$$

Here θ is the azimuthal angle between the in-plane momentum wavevector k_{\parallel} and the a -axis direction of the crystal, as shown in Fig. 1. This is a simple model which nevertheless allows us to explore the transition from isotropic ($\Gamma_f = \Gamma_s$) to extremely anisotropic scattering ($\Gamma_f \gg \Gamma_s$). The latter limit corresponds to the case studied by Ioffe and Millis, where, at the planar zone diagonals [$\theta = (2n + 1)\pi/4$] the scattering rate has a minimum. In their model, Γ_s is just the Fermi-liquid scattering rate, $\Gamma_s = 1/\tau_{FL} \sim T^2$. The scattering around the Fermi-surface in the limit of strong anisotropy is illustrated in Fig. 2.

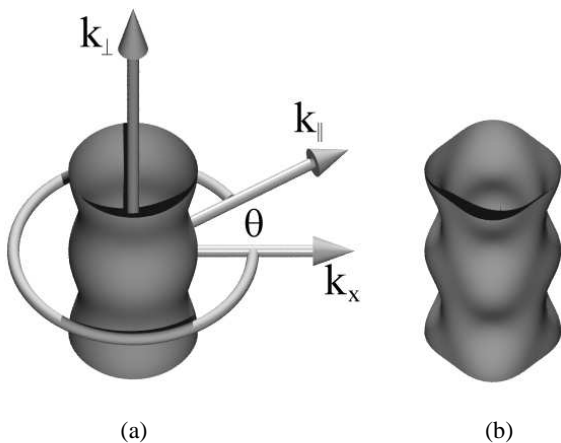


FIG. 1: The cylindrical coordinates used in this paper. This also illustrates the Fermi surface we consider with the c -axis dispersion greatly exaggerated. The degree to which the c -axis dispersion depends on the in-plane momentum varies within this model from (a) no dependence ($\gamma = 0$) to (b) the case when there is no dispersion along the zone diagonals ($\gamma = 1$).

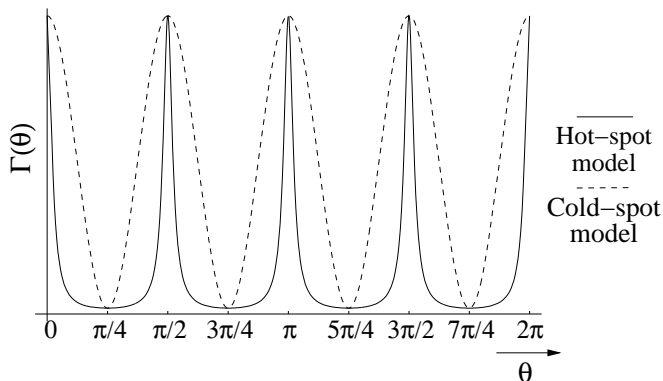


FIG. 2: The angular dependence of the scattering rate in our parameterization of the cold-spot model (dotted line and Eq. 1) and the hot-spot model (solid line and Eq. 5). Although the current is preferentially carried by the longest-lived quasiparticle, in the cold-spot model the short-lived particles can contribute since they cover most of the Fermi line. In the hot-spot model the cold regions short circuit all transport processes and dominate all quantities.

It will often be convenient to express the scattering rate in terms of an anisotropy parameter, α , where Eq. 1 is written as

$$\Gamma(k_{\parallel}, \theta, k_{\perp}) = \Gamma_0(1 + \alpha \cos 4\theta), \quad (2)$$

with

$$\Gamma_0 = (\Gamma_f + \Gamma_s)/2, \quad (3)$$

$$\alpha = \frac{(\Gamma_f - \Gamma_s)}{(\Gamma_f + \Gamma_s)}. \quad (4)$$

In this form $\alpha = 0$ gives us the isotropic scattering case whilst $\alpha = 1$ or -1 gives large anisotropy with cold spots on the zone diagonals or zone axes respectively. We will express results in either notation (Γ_f, Γ_s or α, Γ_0) depending on applicability to available data and ease of interpretation, and are always able to calculate across the full range of α .

B. The hot-spot model

Alternatively it has been proposed that hot spots exist near the $(\pi, 0)$ points of the Brillouin zone where strong scattering occurs, perhaps due to antiferromagnetic spin fluctuations. This leaves quasiparticles on the rest of the Fermi surface with a longer lifetime. To capture this within our phenomenology we add the scattering lifetimes around the Fermi surface so

$$\Gamma_{\mathbf{k}}^{-1} = \tau(k_{\parallel}, \theta, k_{\perp}) = \tau_f \cos^2 2\theta + \tau_s \sin^2 2\theta. \quad (5)$$

Here we expect τ_f to be smaller than τ_s so that we have a model with strong-scattering hot spots and extended cold regions with less scattering (see Fig. 2).

C. Bandstructure

The next component of the model is the bandstructure. We assume that the in-plane dispersion is isotropic, which is not unreasonable for the cuprates. By contrast the dispersion in the out-of-plane direction is known to have significant dependence on the in-plane momentum^{27,28,29}. This is due to the local chemistry of the copper-oxide planes as emphasized by Xiang³⁰. Transport between planes occurs principally through the copper 4s orbitals. Since these orbitals are circularly symmetric in the plane, their overlap amplitude with the Cu $3d_{x^2-y^2}$ -O 2p hybrids has d-wave symmetry as illustrated in Fig. 3. The resulting tunneling term is therefore proportional to the square of this amplitude and can be represented by the form $t_{\perp} \cos^2(2\theta)$. The most important effect this has on c -axis transport stems from the fact that the longest-lived quasiparticles on the zone diagonals are precisely those that have a vanishing probability of c -axis hopping. For this reason we ignore other features of the c -axis dispersion which may lead to additional small tunneling probabilities at other points on the Fermi-surface such as those due to a body-centered tetragonal unit cell considered elsewhere^{18,31}. Our bandstructure is then given by

$$\epsilon(\mathbf{k}_{\parallel}, \theta, \mathbf{k}_{\perp}) = \epsilon(k_{\parallel}^2) - 2t_{\perp}(1 + \gamma \cos 4\theta) \cos(k_{\perp}c). \quad (6)$$

To illustrate the importance of this effect and to allow for other tunneling mechanisms we parameterize the degree of tunneling anisotropy by γ , which we allow to vary from 0 to 1. When $\gamma=1$, we have complete elimination

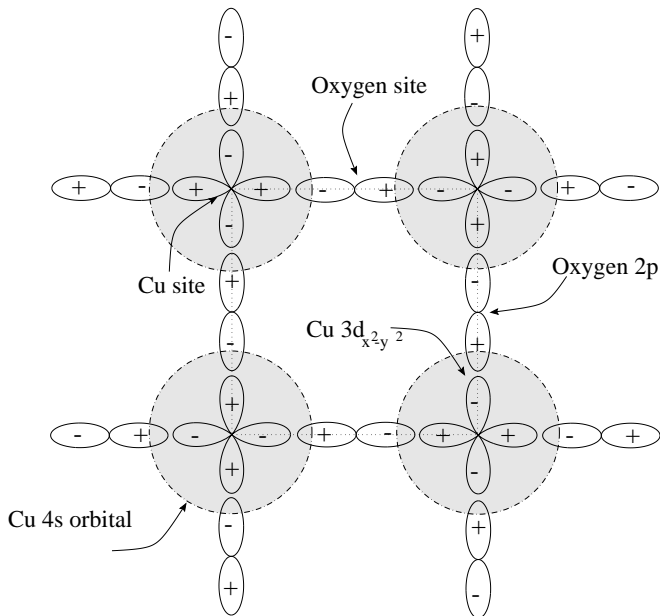


FIG. 3: The overlap between the hybrids of copper $3d_{x^2-y^2}$ and oxygen 2p orbitals and a copper 4s has d-wave symmetry. Since transport between layers occurs primarily via the copper 4s orbitals, the c -axis tunneling probability vanishes when the in-plane quasiparticle momentum is directed along the zone diagonals—the zeros of the $d_{x^2-y^2}$ form (after Xiang *et al.*³⁰).

of c -axis transport for quasiparticles with in-plane momentum along the zone diagonals. The frequency dependence of this end-point of the model has been studied by van der Marel¹⁸. Allowing both the degree of scattering anisotropy (α) and c -axis dispersion (γ) to vary across their full range turns out to be crucial in understanding the out-of-plane transport and is a novel aspect of this work. It unifies various other approaches^{13,17,25} which focus on the extremes of one or other of the ranges of α and γ .

III. RESULTS

Using the standard representation of the quasiparticle distribution, $f = f^{(0)} + \psi \partial_\epsilon f^{(0)}$, we write the Boltzmann equation (for uniform fields and temperature gradients) as³²

$$-\partial_t \psi + \Gamma_{\mathbf{k}} \psi - \frac{e}{\hbar} (\mathbf{E} + \mathbf{v}_{\mathbf{k}} \times \mathbf{B}) \cdot \nabla_{\mathbf{k}} \psi = e \mathbf{E} \cdot \mathbf{v}_{\mathbf{k}} - \frac{\epsilon_{\mathbf{k}} - \mu}{T} \mathbf{v}_{\mathbf{k}} \cdot \nabla(T)$$

We will solve this equation in various limits in the subsequent sections. We will only be interested in d.c. properties in this paper, however our results for the cold-spot model (Eq. 1) are easily extended into the frequency domain. After Fourier transforming with respect to time, we see that

$$-\partial_t \psi + \Gamma(\theta) \psi \rightarrow i\omega \psi + (\Gamma_f \cos^2 2\theta + \Gamma_s \sin^2 2\theta),$$

$$\rightarrow (\Gamma_f + i\omega) \sin^2 2\theta + (\Gamma_s + i\omega) \cos^2 2\theta. \quad (8)$$

We can therefore obtain the finite frequency results for the cold-spot model from our expressions at d.c. simply by the prescription

$$\Gamma_f \rightarrow \Gamma_f + i\omega, \quad \Gamma_s \rightarrow \Gamma_s + i\omega. \quad (9)$$

A. In-plane transport in weak magnetic fields

We first focus on leading order response in an in-plane electric field. For a circular Fermi surface we may write Eq. 7 as

$$\Gamma(\theta) \psi - \omega_c \frac{\partial \psi}{\partial \theta} = eE v_F \cos \theta, \quad (10)$$

where $\omega_c = eB v_F / (\hbar k_F)$ and v_F is the in-plane Fermi velocity.

We may solve this equation by Jones-Zener expansion for in-plane currents with a weak magnetic field along the c -axis. The currents, and hence conductivity elements are calculated using the relation

$$\mathbf{j}_\mu = \frac{eE}{4\pi^3 \hbar} \int \int \frac{\mathbf{v}_\mu k_F}{v_F} \psi d\theta dk_\perp, \quad (11)$$

where current is flowing in direction μ with velocity \mathbf{v}_μ . We expand σ_{xx} and σ_{xy} to order B^2 and the resistivity is then found by simple matrix inversion.

If we consider first hot-spot scattering (Eq. 5), we can see that this scattering rate can be eliminated as a viable model for the cuprates. Each of the properties evaluated is dominated by the long scattering time, which is the short-circuiting effect proposed by Hlubina and Rice¹⁶. The in-plane conductivities are given by

$$\sigma_{xx}^{(0)} = \frac{e^2 k_F v_F (\tau_f + \tau_s)}{4\pi \hbar c}, \quad (12)$$

$$\frac{\sigma_{xy}}{\sigma_{xx}^{(0)}} = \tan \Theta_H = \omega_c \frac{(3\tau_f^2 + 2\tau_f \tau_s + 3\tau_s^2)}{4(\tau_f + \tau_s)} + O[B^3], \quad (13)$$

$$\frac{\Delta \sigma_{xx}}{\sigma_{xx}^{(0)}} = -\omega_c^2 \frac{(21\tau_f^2 - 34\tau_f \tau_s + 21\tau_s^2)}{8} + O[B^4]. \quad (14)$$

Within this model, all computed quantities are dominated by τ_s in the limit of strong anisotropy ($\tau_s \gg \tau_f$). This model is unable to reproduce the two-lifetime phenomenology of the cuprates so we will not consider it further.

However, for the cold spot model we obtain the following in terms of Γ_f and Γ_s :

$$\sigma_{xx}^{(0)} = \frac{e^2 v_F k_F}{2\pi \hbar c} \frac{1}{\sqrt{\Gamma_f \Gamma_s}}, \quad (15)$$

$$\frac{\sigma_{xy}}{\sigma_{xx}^{(0)}} = \tan \Theta_H = \frac{\omega_c}{2} \left(\frac{1}{\Gamma_f} + \frac{1}{\Gamma_s} \right) + O[B^3], \quad (16)$$

Quantity	Cold-spot model	Experiment	Reference
$\rho_{xx}^{(0)}$	$\sqrt{\Gamma_f \Gamma_s}$	T	2
$\cot \Theta_H$	$\frac{2\Gamma_s}{\omega_c}$	T^2	4
$\frac{\Delta\rho_{xx}}{\rho_{xx}^{(0)}}$	$\omega_c^2 \frac{\Gamma_f}{\Gamma_s^3}$	Θ_H^2	7
$\frac{1}{\Theta_H^2} \frac{\Delta\rho_{xx}}{\rho_{xx}^{(0)}}$	$\frac{\Gamma_f}{\Gamma_s}$	const	7

TABLE I: A comparison of our results with experiment in the limit of highly-anisotropic scattering.

$$\frac{\Delta\rho_{xx}}{\sigma_{xx}^{(0)}} = \omega_c^2 \left[\frac{5}{8} \left(\frac{\Gamma_f}{\Gamma_s^3} + \frac{\Gamma_s}{\Gamma_f^3} \right) - \frac{1}{8} \left(\frac{1}{\Gamma_f^2} + \frac{1}{\Gamma_s^2} \right) \right] + O[B^4]. \quad (17)$$

This results in an in-plane orbital weak-field magnetoresistance

$$\frac{\Delta\rho_{xx}}{\rho_{xx}^{(0)}} = \omega_c^2 \frac{(\Gamma_f - \Gamma_s)^2}{8\Gamma_f^3\Gamma_s^3} (5\Gamma_f^2 + 7\Gamma_f\Gamma_s + 5\Gamma_s^2), \quad (18)$$

which vanishes in the isotropic limit ($\Gamma_s = \Gamma_f$). This reflects the well known result that there is no orbital magnetoresistance in an isotropic metal. In the high anisotropy ($\alpha \rightarrow 1$) limit, where $\Gamma_f \gg \Gamma_s$, we find the results shown in table I.

These results illustrate the way in which the cold-spot model reproduces the phenomenology of the cuprates as shown by Ioffe and Millis¹⁷. They take Γ_f to be large and temperature independent, while Γ_s is assumed small and proportional to T^2 . The geometric mean then gives the linear in temperature resistivity while the inverse Hall angle is proportional to Γ_s and hence varies as T^2 . The results are also illustrative of the problems of this model. Adding Zn impurities to the CuO_2 has been interpreted as adding a unitary scatterer which should add a temperature independent term to the scattering rates. Adding a constant elastic scattering term to the two rates appearing in the geometric mean which forms the resistivity (Eq. 15) will not reproduce the Matthiessen's rule behavior seen in experiment⁴. Instead it will change both the temperature dependence and the intercept of the resistivity.

The second difficulty is the large magnetoresistance that this model predicts. While experiments suggest that the magnetoresistance is proportional to the Hall angle squared⁷ with a constant of proportionality which can be of order 1, the cold-spot model predicts that these two quantities differ by Γ_f/Γ_s —a large, temperature dependent factor. It is tempting to appeal to new physical processes to explain this (such as vertex corrections). However the cause of this large magnetoresistance is intimately related to the appearance of distinct temperature dependences of the resistivity and inverse Hall angle. Magnetic fields couple to the anisotropy of ψ around the Fermi surface as can be seen from Eq. 10 and so at each order in the magnetic field, the effect of the anisotropy in the model is amplified. This allows the inverse Hall angle to differ from the resistivity but consequently has

an even more dramatic effect on the magnetoresistance which is higher order in magnetic field. We do not attempt to offer a solution for this puzzle though given the systematics in transport behavior across a wide range of cuprates it seems unlikely that this is due to fine tuning. (By contrast in the charge-conjugation phenomenology⁸ the magnetoresistance is proportional to the square of the Hall angle and is small since this model is isotropic around the Fermi surface.)

B. Beyond the weak-field regime

Thus far, in keeping with other workers, we have shown that in-plane transport is governed by a different scattering rate (formed from the combination of Γ_f and Γ_s) at each order in the magnetic field. Here we go beyond the weak-field regime and show numerically that no new combinations emerge beyond second order in the magnetic field until the magnetoresistance saturates. The scattering rate combination for weak-field magnetoresistance provides the scale for magnetic field effects throughout the intermediate field region.

The saturation field may be obtained from a high field expansion of the Boltzmann equation—expanding the solution in powers of $1/\omega_c$. We find that the magnetoresistance saturates at a value of

$$\frac{\Delta\rho_{xx}(B \rightarrow \infty)}{\rho_{xx}(B = 0)} = \frac{(\sqrt{\Gamma_f} - \sqrt{\Gamma_s})^2}{2\sqrt{\Gamma_s\Gamma_f}}. \quad (19)$$

The high field limit is reached when $\omega_c \sim \Gamma_f$ so the fastest rate controls the transition to the high field limit. This is because saturation requires that quasiparticles can completely orbit the Fermi surface and it is the hot regions which limit this process³³. This is also the scale for Landau quantization. The approach to the saturated value is shown in Fig. 4. The magnetic field is plotted as a function of ω_c/Γ_0 since in the cold spot model this is dominated by Γ_f and so shows that this sets the scale for saturation.

[As an aside, we can obtain the universal form of the magnetoresistance in an isotropic metal. Of course, this is formally zero but by dividing by the saturated value in the limit of small anisotropy we can obtain a finite result. This is also shown in Fig. 4.]

While we cannot solve Eq. 10 analytically except in the low and high field limits, the equation is readily solved numerically. The fact that we require a solution of ψ which is periodic around the Fermi surface means that we can look for a Fourier series solution. Our numerical results reproduce the analytical results of the previous section. In addition, we find the remarkable result that the magnetoresistance is a function of a single dimensionless parameter until it saturates. This scaling parameter governs the magnetoresistance even beyond the weak-field (B^2) regime of the magnetoresistance so we

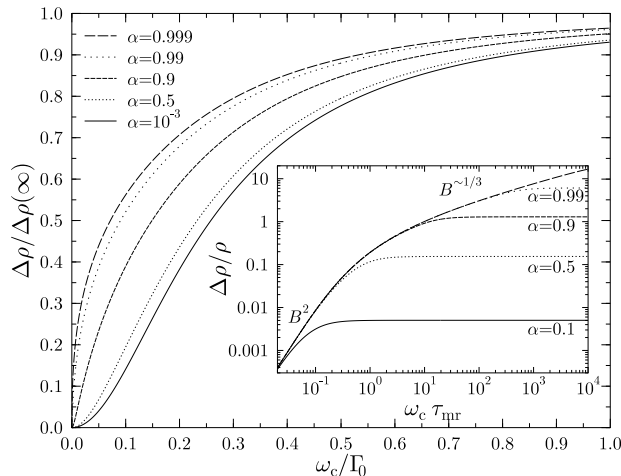


FIG. 4: The in-plane magnetoresistance is shown beyond the weak field region as determined from a numerical solution. Saturation occurs at a scale determined by $\omega_c \sim \Gamma_0$ since quasiparticles must precess around the whole Fermi surface. The inset shows that no new field scale emerges between the weak-field and the saturated regime. By scaling the data to the weak-field region (thereby defining τ_{mr}) we see that the magnetoresistance continues to fall on a universal curve beyond the B^2 regime until the saturated magnetoresistance value is reached.

may write

$$\frac{\Delta\rho_{xx}(B)}{\rho_{xx}(0)} = f(\omega_c\tau_{mr}), \quad \omega_c \ll \Gamma_f, \quad (20)$$

where τ_{mr} is defined by the weak-field magnetoresistance such that $\Delta\rho_{xx}/\rho_{xx} = (\omega_c\tau_{mr})^2$. For $\Gamma_f \gg \Gamma_s$ we have $\tau_{mr}^2 \sim 5\Gamma_f/8\Gamma_s^3$.

We illustrate this universality in the inset to Fig. 4. We see that as a function of this combination of scattering rates, the magnetoresistance follows a universal curve until the saturation value is approached. An intermediate field region emerges for fields $1 < \omega_c\tau_{mr} < \omega_c/\Gamma_f$, where the magnetoresistance adopts a new power law $\sim B^{0.33}$. Thus our numerical treatment suggests that no new scattering rate combinations are produced in the Jones-Zener expansion until the magnetoresistance saturates. We have confirmed this is the case analytically at fourth order in the magnetic field. This scaling also means that in our model there is an absolute value of magnetoresistance above which one must see a deviation from a B^2 dependence. Our model predicts that with a magnetoresistance of only 0.5% one would expect at least a 10% deviation from a B^2 form. Comparing this with experimental work³³ on optimally doped Tl-2201 in pulsed magnets, we find a deviation from quadratic dependence is only perhaps being seen in optimally doped Tl-2201 at a magnetoresistances of order 3%. (The observed deviation from the weak-field region is more consistent with the Coleman-Schofield-Tsvetlik phenomenology which predicts that this should occur when the mag-

netoresistance is at or less than about 10%³³.)

C. c -axis transport

In-plane magnetoresistance in the cold-spot model is at odds with the current experiments. It has been argued that including vertex corrections could correct this^{22,23}. As we have argued in the introduction, c -axis transport is then of fundamental importance in testing the cold-spot model. This is because to lowest order in t_{\perp}^2 the c -axis conductivity is related to the convolution of two in-plane spectral functions³⁴. These are the quantities which may be inferred from the angle-resolved photoemission that inspired the cold-spot model. Thus, independent of a picture of quasiparticles for in-plane transport, a cold-spot model should be able to account for the c -axis d.c. conductivity²⁴. In particular we must show that this leads to a consistent picture of c -axis orbital magnetoresistance (magnetic field in the plane and electric field out of the plane). The most systematic study of these effects has been performed by Hussey *et al.*²⁵ in overdoped Tl-2201 and this motivates the following analysis. The two-lifetime behavior is much less apparent in the overdoped material so we will not be able to use the $\Gamma_f \gg \Gamma_s$ asymptotics. Instead we need a full solution for any degree of anisotropy.

We will now calculate the c -axis magnetoresistance, $\Delta\rho_{zz}/\rho_{zz}$. To obtain this, we first calculate the relevant components of the conductivity matrix, σ_{ij} and invert. In this experimental geometry, σ has zero components $\sigma_{xy}, \sigma_{xz}, \sigma_{yx}$ and σ_{zx} due to the \mathbf{B} field being in-plane. σ_{xx} is equal to the zero-magnetic field value of σ_{yy} . We can expand the other terms in magnetic field:

$$\sigma_{\nu\mu} = \sigma_{\nu\mu}^{(0)} + \sum_{n=1}^{n=3} \sigma_{\nu\mu}^{(n)}, \quad (21)$$

where the superscripts refer to the order of effect in magnetic field. Symmetry under time reversal means, of course, that $\sigma_{zz}^{(1)}$ and $\sigma_{zz}^{(3)}$ and the Hall terms $\sigma_{yz}^{(0)}$ and $\sigma_{yz}^{(2)}$ are zero. In addition the Hall term $\sigma_{yz}^{(1)}$ is small ($\sim t_{\perp}^2$). Under these conditions, the c -axis magnetoresistivity in weak magnetic field simplifies to

$$\begin{aligned} \rho_{zz} &= \rho_{zz}^{(0)} + \Delta\rho_{zz}^{(2)} - \Delta\rho_{zz}^{(4)} + O[B^6], \\ \frac{\Delta\rho_{zz}^{(2)}}{\rho_{zz}^{(0)}} &= -\frac{\sigma_{zz}^{(2)}}{\sigma_{zz}^{(0)}}, \\ \frac{\Delta\rho_{zz}^{(4)}}{\rho_{zz}^{(0)}} &= -\frac{(\sigma_{zz}^{(2)} - \sigma_{zz}^{(0)}\sigma_{zz}^{(4)})}{\sigma_{zz}^{(0)2}}. \end{aligned} \quad (22)$$

Here we have adopted the sign convention of Hussey *et al.*²⁵ and Drăgulescu *et al.*³¹, expecting the fourth-order magnetoresistivity to be negative.

To obtain the conductivity, we follow the same general procedure as for the in-plane case, solving the Boltzmann

equation using a Jones-Zener expansion. We now introduce the angle, ϕ , which is the in-plane angle between the B field and the a -direction. θ becomes the azimuthal coordinate relative to the direction of the B field. The solutions to the Boltzmann equation are now

$$\psi(\mathbf{k}) = \frac{eE}{\hbar\Gamma(\theta + \phi)} \frac{\partial\epsilon}{\partial k_{\perp}} + \sum_{n=1}^{\infty} \psi^{(n)}(\mathbf{k}), \quad (23)$$

where, to lowest order in t_{\perp} ,

$$\psi^{(n)}(\mathbf{k}) = -\frac{eB^n}{\hbar\Gamma(\theta + \phi)} \left(\frac{1}{\hbar} v_F \sin\theta \frac{\partial\psi^{(n-1)}}{\partial k_{\perp}} \right). \quad (24)$$

The ratio of $\sigma_{zz}^{(2)}/\sigma_{zz}^{(0)}$, when expanded in powers of α yields a zero-order term which is, as Hussey *et al.*²⁵ first showed

$$\frac{\sigma_{zz}^{(2)}}{\sigma_{zz}^{(0)}} = -\frac{c^2 e^2 v_F^2}{2\hbar^2 \Gamma_0^2} + O[\alpha^2]. \quad (25)$$

Similarly, for the quadratic term in the c -axis conductivity:

$$\frac{\sigma_{zz}^{(4)}}{\sigma_{zz}^{(0)}} / \left(\frac{\sigma_{zz}^{(2)}}{\sigma_{zz}^{(0)}} \right)^2 = \frac{6 + 3\gamma^2 + 2\gamma \cos(4\phi)}{2(2 + \gamma^2)}, \quad (26)$$

which in the limit of simple inter-plane tunneling ($\gamma \rightarrow 0$) gives 3/2, again as shown by Hussey *et al.*

The Hall conductivity, σ_{yz} , is found to vary as t_{\perp}^2 . In the limit of isotropic in-plane scattering the out-of-plane Hall angle is identical to the in-plane one³⁵

$$\lim_{\alpha \rightarrow 0} \frac{\sigma_{yz}^{(1)}}{\sigma_{zz}^{(0)}} = \frac{eBv_F}{\hbar k_F \Gamma_0}. \quad (27)$$

This is not true in general however. Nevertheless its dependence on t_{\perp}^2 means that the Hall conductivity does not appear, at leading order, in the out-of-plane magnetoresistance.

Rather than display the full expression for every quantity we have calculated, we show graphically two quantities which Hussey *et al.* examined experimentally in single-crystal $\text{Tl}_2\text{Ba}_2\text{CuO}_6$. There a key observation was the four-fold variation of the c -axis magnetoresistance as the magnetic field was rotated in-plane, *i.e.* that

$$\Delta\rho_{zz}^{(4)} = \tilde{\rho}_{zz}^{(4)} + \tilde{\rho}_{zz}^{(4)} \cos(4\phi), \quad (28)$$

where $\tilde{\rho}_{zz}^{(4)}$ and $\tilde{\rho}_{zz}^{(4)}$ were both found to be positive. In fact it is straightforward to show that this 4-fold modulation at fourth order in B is a simple consequence of square symmetry. Hussey *et al.* initially analyzed their angle-dependent magnetoresistance results purely in terms of anisotropic, in-plane scattering (as parameterized here by α). We first look at the offset part in the fourth order magnetic field term in the magnetoresistance. We examine $\frac{\tilde{\rho}_{zz}^{(4)}/\rho_{zz}^{(0)}}{(\Delta\rho_{zz}^{(2)}/\rho_{zz}^{(0)})^2}$, a quantity found experimentally to be

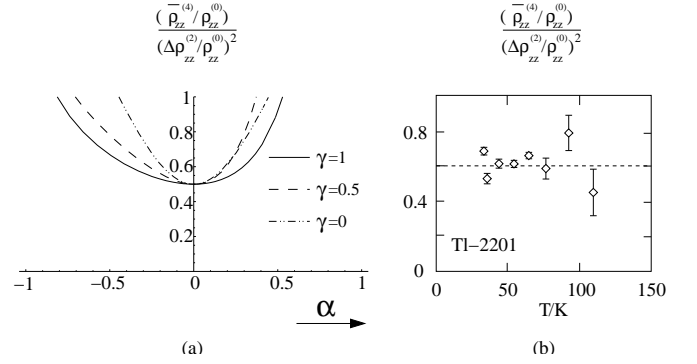


FIG. 5: (a) $\frac{\tilde{\rho}_{zz}^{(4)}/\rho_{zz}^{(0)}}{(\Delta\rho_{zz}^{(2)}/\rho_{zz}^{(0)})^2}$ and (b) experimental data²⁵ from measurements on $\text{Tl}_2\text{Ba}_2\text{CuO}_6$, where this quantity was 0.6 ± 0.1 , approximately independent of temperature. This implies that α should not vary greatly in the experimental range of temperatures.

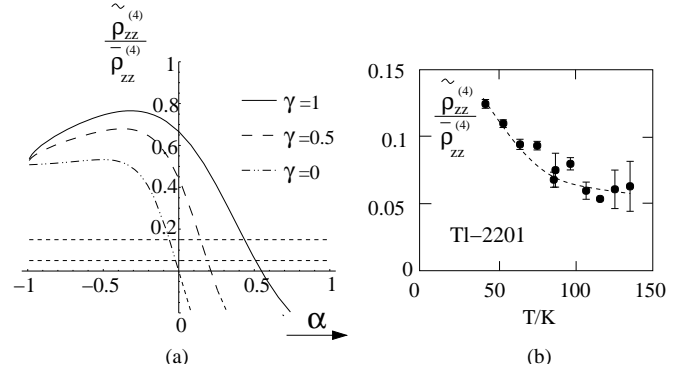


FIG. 6: (a) The size of the fourth order modulation in c -axis magnetoresistance, relative to the offset at this order and (b) experimental data²⁵ from measurements on $\text{Tl}_2\text{Ba}_2\text{CuO}_6$ again shown for comparison. A positive value of $\tilde{\rho}_{zz}^{(4)}/\tilde{\rho}_{zz}^{(4)}$ means that resistance maxima exist for a magnetic field along [110]. The effect of bandstructure is therefore pronounced and produces resistance maxima where the cold spots are on the zone diagonals ($\alpha > 0$). In (a), the approximate constraints on the valid regions of (α, γ) parameter space are given by the limits of the modulation as taken from experiment. These are shown as dotted lines at values of 0.15 and 0.05.

roughly independent of temperature and approximately equal to 0.6 (0.6 ± 0.1). We show it for various values of γ , as a function of α in Figure 5. This puts a constraint on the temperature dependence of α , an issue which is explored in section IV where we try to fit magnetoresistance data to our model.

The second quantity studied experimentally is the amplitude of the modulation in magnetoresistance at order B^4 . The quantity evaluated is $\tilde{\rho}_{zz}^{(4)}/\tilde{\rho}_{zz}^{(4)}$, which is positive when the resistance is maximum with \mathbf{B} aligned along the zone diagonal (Eq. 28). This too is plotted across the range of scattering anisotropy, α , for various bandstructures, γ , in Figure 6.

Hussey *et al.* found it to vary with temperature, drop-

ping from about 0.15 at 50K to 0.05 at about 140K, and these limits are shown as dotted lines in Figure 6. In our calculations, $\tilde{\rho}_{zz}^{(4)}/\bar{\rho}_{zz}^{(4)}$ is positive when α is negative, corresponding to a situation where the hot spots and cold spots have effectively exchanged their usual positions. This can be explained intuitively by identifying the maxima in the Lorentz force, $\mathbf{v} \times \mathbf{B}$, at points on the Fermi surface orthogonal to the in-plane magnetic field. Then, loosely, the parts of the Fermi surface least affected by a magnetic field are those with \mathbf{v}_F parallel to \mathbf{B} . Thus, naively, one would expect the *minima* in the magnetoresistance to occur when the field is along the cold-spot directions. In fact experimentally this orientation gives a maxima in the magnetoresistance. Turning on anisotropy in the c -axis dispersion γ , one can sufficiently inhibit c -axis transport through the cold spots in the *positive* α regime that resistance maxima can be seen for \mathbf{B} along [110] with cold spots along [110] in keeping with the experiments.

This effect has been attributed elsewhere³¹ to the curvature of the real Fermi surface in a model of isotropic scattering. Here we have shown that the two effects will work together in the regime of positive bandstructure anisotropy. Once again, however, we see that there is a constraint on the allowed degree of variation of scattering anisotropy with temperature. In Table II we show the form of these 4th order quantities shown in Figures 5 and 6 as well as the size of the 2nd order magnetoresistivity and in-plane properties. This will be useful when fitting to data later.

D. Non-ohmic conductivity

We have also calculated the non-ohmic, in-plane conductivity of the system in zero magnetic field. Hlubina³⁶ has suggested that this is a useful test of the model of Ioffe and Millis. The Boltzmann equation (Eq. 7) is now solved by Jones-Zener expansion in \mathbf{E} and is given by

$$\Gamma_{\mathbf{k}}\psi - \frac{e}{\hbar}\mathbf{E} \cdot \nabla_{\mathbf{k}}\psi = e\mathbf{E} \cdot \mathbf{v}_{\mathbf{k}}. \quad (29)$$

From the 4-fold symmetry of the system, it is straightforward to deduce that the currents in the x and y directions must have the following form at third order in the electric field:

$$j_x = \sigma_0 E_x + \sigma_1 E_x^3 + \sigma_2 E_y^2 E_x, \quad (30)$$

$$j_y = \sigma_0 E_y + \sigma_1 E_y^3 + \sigma_2 E_x^2 E_y. \quad (31)$$

We then find that

$$\sigma_0 = \frac{e^2 k_F v_F}{2\pi \hbar c \Gamma_0 (1 - \alpha^2)^{1/2}}, \quad (32)$$

$$\sigma_1 = -\frac{e^4 v_F}{4\pi \hbar^3 k_F c \Gamma_0^3} \frac{\alpha((1 + \alpha)(\alpha^2 + 2\alpha + 2))}{(1 - \alpha^2)^{7/2}}, \quad (33)$$

$$\sigma_2 = -\frac{e^4 v_F}{4\pi \hbar^3 k_F c \Gamma_0^3} \frac{\alpha(\alpha^3 - 9\alpha^2 + 4\alpha - 6)}{(1 - \alpha^2)^{7/2}}, \quad (34)$$

which all simplify or reduce to zero appropriately in the isotropic limit, $\alpha \rightarrow 0$. Furthermore, in the limit of strong anisotropy, $\alpha \rightarrow 1$, we find $\sigma_1 = -\sigma_2$, as demonstrated by Hlubina³⁶.

The most obvious consequence of non-linear response in the electric field is that the current no longer flows parallel to the electric field. Defining the parallel current (j_{\parallel}) as being the response parallel to the applied field, and the transverse current as the current component perpendicular to the applied field (j_{\perp}) we find that

$$j_{\perp} = \frac{1}{4} E^3 (\sigma_1 - \sigma_2) \sin 4\phi, \quad (35)$$

where ϕ is the angle between the in-plane electric field and the a -axis. Using our expressions for σ_1 and σ_2 (Eqs. 33 and 34) we may write

$$\frac{j_{\perp}}{j_{\parallel}} = \left(\frac{eE}{\hbar k_F \Gamma_0} \right)^2 \frac{\alpha(2 + \alpha^3)}{2(1 - \alpha^2)^3} \sin 4\phi, \quad (36)$$

$$= \lim_{\alpha \rightarrow 1} \left(\frac{v_d}{v_F} \right)^2 \frac{5}{16} \left(\frac{\Gamma_f}{\Gamma_s} \right)^3 \sin 4\phi. \quad (37)$$

Here $v_d = eE/2m\Gamma_0$ is the Drude drift velocity of a fast decaying quasiparticle. So, although the v_d/v_F is generally tiny, nonlinear effects are indeed strongly enhanced by anisotropy.

E. Thermal transport

In this treatment we have not speculated on the anisotropy of the energy relaxation rate around the Fermi surface. However if we make the assumption that the energy relaxation follows the quasiparticle relaxation rate and only varies around the Fermi surface (as opposed to variations away from the Fermi surface) we can calculate all of the thermal transport coefficients. Without reproducing the details of the calculation we can see immediately from the form of the Boltzmann equation (Eq. 7) that temperature gradients drive the quasiparticle distribution in exactly the same way as electric fields except for the usual factor of $(\epsilon_{\mathbf{k}} - \mu_F)/T$. This is seen in the right-hand-side of Eq. 7. This factor is isotropic around the Fermi surface and does not introduce any further angular dependence. Thus we can conclude that all currents proportional to temperature gradients will have exactly the same dependence on scattering rate as those driven by electric fields (for example $\sqrt{\Gamma_f \Gamma_s}$ in the absence of a magnetic field). Within this approximation the thermal conductivity will obey the Wiedemann-Franz law and the diffusion thermopower will have the usual linear temperature dependence and be independent of the scattering rate. To account for the unusual systematics in the measured thermopower of the cuprate metals³⁷ in this model one would need to add a significant anisotropic energy dependence of the scattering rate that differs from the anisotropy of the transport relaxation rate.

Quantity	$\rho_{xx}^{(0)}$	$\cot \Theta_H$	$\frac{\Delta\rho_{xx}^{(2)}}{\rho_{xx}^{(0)}}$	$\Delta\rho_{xx}^{(2), (0)}$	$\frac{\Delta\rho_{zz}^{(2)}}{\rho_{zz}^{(0)}}$	$\frac{(\tilde{\rho}_{zz}^{(4)}/\rho_{zz}^{(0)})}{(\Delta\rho_{zz}^{(2)}/\rho_{zz}^{(0)})^2}$	$\tilde{\rho}_{zz}^{(4)}/\tilde{\rho}_{zz}^{(4)}$
Cold-spot model	$\frac{2\pi\hbar c\Gamma_0}{c^2 v_F k_F} (1 - \alpha^2)^{1/2}$	$\frac{\hbar k_F \Gamma_0 (1 - \alpha^2)}{e B v_F}$	$(\frac{e B v_F}{\hbar k_F \Gamma_0})^2 \frac{\alpha^2 (17 + 3\alpha^2)}{2(1 - \alpha^2)^3}$	$(\frac{2\pi c B}{k_F^2 e})^2 \frac{\alpha^2 (17 + 3\alpha^2)}{2(1 - \alpha^2)^2}$	$(\frac{c e v_F B}{\hbar \Gamma_0})^2 f_1(\alpha, \gamma)$	$f_2(\alpha, \gamma)$	$f_3(\alpha, \gamma)$

TABLE II: Results of our calculations of in-plane and c -axis properties. In particular we have attempted to find dimensionless quantities, f_1 , f_2 and f_3 , which are functions of α and γ . This enables us to constrain the values of α and γ by comparing directly to experiments without further assumptions.

IV. APPLICATION TO EXPERIMENTAL DATA

In order to apply the analytic results of our model to experimental data, we have made a comparison of magnetoresistivity results with measurements on overdoped samples of single-crystal $\text{Tl}_2\text{Ba}_2\text{CuO}_6$, made by Tyler³⁸ and Hussey²⁵. We choose this system because its c -axis magnetoresistance is well characterized. We have argued that c -axis properties are the most robust quantities in this model since they are not affected by vertex corrections, nor do they rely on a quasiparticle picture. We then identify combinations of measured c -axis quantities which directly probe the degree of anisotropy with minimal dependence on unknown parameters. Finally we address the in-plane transport features. We also identify combinations of experimental quantities which allow a comparison with theory involving the fewest assumptions on unknown parameters. In particular we can constrain the degree of anisotropy in the c -axis dispersion (γ) and the range of scattering anisotropy (α) from the c -axis magnetoresistance.

First we consider the overall magnitude of the fourth order magnetoresistance by comparing this to the second order term. This is shown in Fig. 5(b). When we compare this to our model [Fig. 5(a)] we see that to obtain the observation of an essentially temperature independent result of around 0.6, the degree of scattering anisotropy must be limited to $\alpha < 0.5$. Furthermore, if α is to have any temperature dependence at all then γ should be approaching 1 where the gradients in Fig. 5(a) are smallest.

We have already remarked on a second conclusion from a comparison between theory and experiment. In order for the maxima in the c -axis magnetoresistance to occur when the field is along the zone-diagonals, c -axis transport along these directions must be suppressed. This is illustrated in Fig. 6(a) where we see that with $\alpha > 0$ we require $\gamma > 0$ to obtain a ratio of $\tilde{\rho}_{zz}^{(4)}/\tilde{\rho}_{zz}^{(4)}$ of the correct sign. Furthermore the experimental bounds on this ratio [illustrated in Fig. 6(b)] confirm that the degree of scattering anisotropy (α) must be less than about 0.6. In no sense then are we in the limit of strong anisotropy in this overdoped material.

A further observation comes from the temperature dependence shown in Fig. 6(b). Generically the quantities shown in Figs. 5(b) and 6(b) should be temperature dependent so the observation that only the second of these

has any significant variation with temperature restricts α to vary between about 0.2 and 0.4 with a band structure anisotropy $\gamma \sim 0.9$. Also, in order to fit the trends in the data, we see that the overdoped state must become less anisotropic as the temperature is lowered. Proximity to a zero temperature critical point would suggest the opposite should be true but perhaps here elastic processes are beginning to dominate.

In order to predict other experimental quantities, we then need to know the temperature dependence of Γ_0 . This too can be found from the second order c -axis magnetoresistance, when data is compared with the functional form in table II, here fixing $\gamma = 1$. In addition it can also be independently inferred from the in-plane resistivity but now relying on the assumptions of Boltzman transport theory.

With these two temperature dependencies known, we may try to predict in-plane properties. We show plots of the cotangent of the Hall angle, $\cot \Theta_H$, and the in-plane magnetoresistance $\Delta\rho_{xx}^{(2)}/\rho_{xx}^{(0)}$, together with experimental data from Hussey and Tyler in Figs. 7 and 8. We see by comparing the experimental data with the parameters extracted from other measurements that the data and theory follow the same trends and are of the correct order of magnitudes. The two different fits on each plot represent the two different methods of inferring Γ_0 : either using the in-plane resistivity or the out-of-plane magnetoresistance. The difference in these two methods is that the in-plane measurements would be expected to be sensitive to the transport lifetime, as opposed to the quasiparticle lifetime in the case of out-of-plane measurements. Surprisingly it appears that the quasiparticle lifetime is longer than the transport lifetime.

Overall we see that for overdoped Tl-2201 a consistent picture emerges of a Fermi-liquid-like metal with weak scattering anisotropy around the Fermi surface but a strong anisotropy in the c -axis dispersion. A more rigorous test of the model would be obtained by performing a similar comparison on optimally doped Tl-2201 ($T_c = 85\text{K}$). There the two-lifetime behavior of in-plane magnetotransport is clearly apparent with very good fits to data being found with simple power laws³⁸:

$$\rho_{xx} = -20 + 1.56(T/\text{K}) \mu\Omega\text{cm}, \quad (38)$$

$$(B/T)\cot \theta_H = 300 + 1.78 * 10^{-2}(T/\text{K})^2, \quad (39)$$

for $100\text{K} < T < 300\text{K}$. In the limit of high in-plane

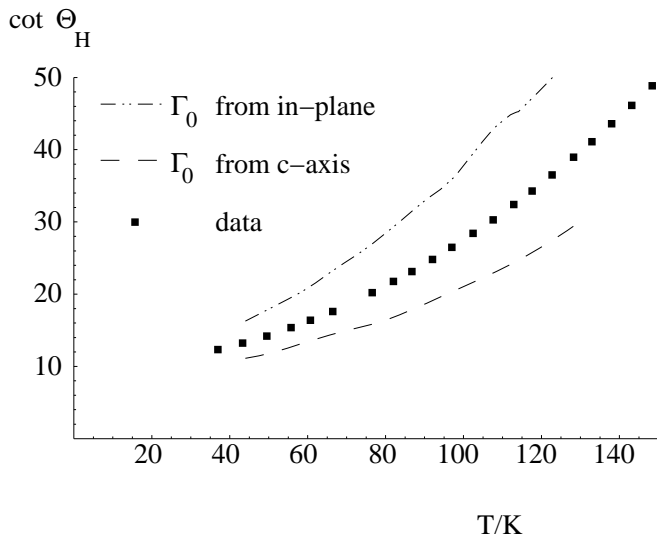


FIG. 7: A comparison of our theoretical prediction for $\cot \Theta_H$ with experimental data³⁸ from measurements on $\text{Tl}_2\text{Ba}_2\text{CuO}_6$. Predictions using Γ_0 found from both in-plane and out-of-plane properties are shown, relating to using the transport or the intrinsic quasiparticle lifetime.

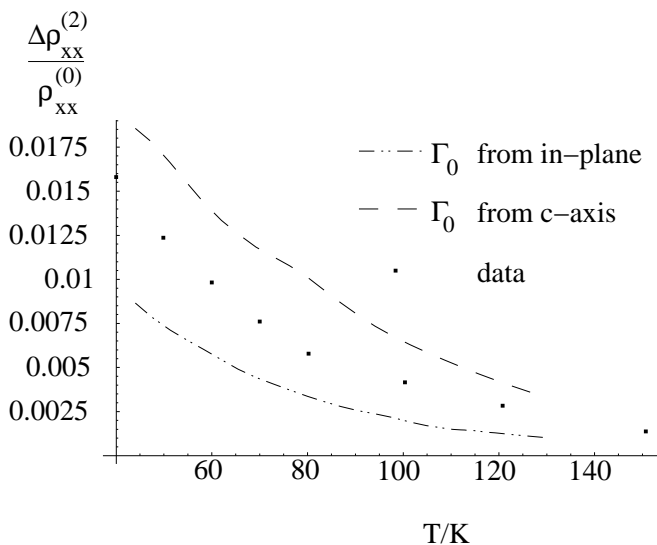


FIG. 8: A comparison of our theoretical prediction for in-plane, second order magnetoresistance with experimental data³⁸ from measurements on $\text{Tl}_2\text{Ba}_2\text{CuO}_6$. Again, predictions using Γ_0 found from both in-plane and out-of-plane properties are shown.

anisotropy we can combine these measurements to obtain the magnetoresistance. We find

$$\frac{\Delta\rho_{xx}}{\rho_{xx}^{(0)}} = \frac{5}{2} \left(\frac{c^2 k_F^4}{\pi^2 c^2 B^2} \right) \left[\frac{\rho_{xx}^{(0)}}{\cot^2 \theta_H} \right]^2. \quad (40)$$

This would predict a magnetoresistance of about 0.04 at 10T and 130K (so already out of the weak-field regime)—a factor of 40 greater than currently seen. We have used

in-plane properties to predict the magnetoresistance so uncertainties about vertex corrections are present in this estimate.

Again, using the in-plane properties, we would expect that the out-of-plane magnetoresistance would be 0.1 in fields as low as 3T with a fourth order magnetoresistance of 0.001 in an in-plane field of about 5T. These effects should be measurable but again rely on using in-plane transport lifetimes to provide a measure of in-plane quasiparticle lifetimes. However, we can make an unambiguous prediction within this model: that the positions of the maxima in resistivity at fourth order should move from the [110] directions (seen in the overdoped system) to the [100] directions in the optimally doped materials. This is seen in Fig. 6(a) where for large α we see that bandstructure is unable to prevent the sign of the modulation term, $\tilde{\rho}_{zz}^{(4)}/\tilde{\rho}_{zz}^{(4)}$, from being negative.

V. CONCLUSION

We have presented a thorough investigation of a minimal model for transport in a quasi-2D system, where we allow for anisotropic scattering in-plane and an anisotropy in the out-of-plane dispersion, both fully variable. Such a model has been proposed for the normal state of the cuprate superconductors with either strong scattering hot spots and weak scattering cold regions around the Fermi surface or hot regions with cold spots. We have studied the transport properties of both types of models and illustrated how short-circuiting in the hot-spot model makes this inconsistent with transport measurements on the cuprates. For the cold-spot model we have computed in- and out-of-plane magnetoresistivity, in-plane non-ohmic conductivity and thermal conductivities for an arbitrary degree of anisotropy.

We find that the in-plane magnetoresistance in this model is too large when compared with experiments on the cuprates, in keeping with other work¹⁷. In addition the in-plane magnetoresistance should be universal beyond the weak field limit with a well defined deviation from a B^2 dependence at weaker fields than currently observed. It has been argued that vertex corrections may account for these discrepancies between the model and experiment. Here we have focussed on the out-of-plane magnetoresistance for which there are no vertex corrections in the quasi-2D limit. We have completely characterized the magnetoresistance to fourth order in this geometry. We have compared our model with experiments on overdoped Tl2201 and show that the model can be reasonably well fit to the experiments. This requires only weak scattering anisotropy but a high degree of bandstructure anisotropy in the c -axis dispersion.

A better test of this model would be to compare it to optimally doped Tl-2201 where the two-lifetime behavior is very clearly seen in in-plane magnetotransport measurements. This model would predict that strong angle dependent c -axis magnetoresistance should be observed

and the positions of the minima in the optimally doped system should be rotated by $\pi/4$ from those of the overdoped material. A quantitative analysis of the degree of in-plane anisotropy could also be made. The extent to which vertex corrections control the in-plane transport properties could then be assessed.

Acknowledgements

The authors would like to thank C. Bergemann, D. R. Broun, N. E. Hussey, S. R. Julian, D. E. Khmel'nitskii,

M. W. Long, G. G. Lonzarich, A. J. Millis, A. Rosch and T. Xiang for useful discussions. We are grateful for the hospitality of the Center for Materials Theory, Rutgers University and the Newton Institute, Cambridge where some of this work was done and also for the support of the Theory of Condensed Matter Group in Cambridge. KGS was funded by the EPSRC, AJS by the Royal Society.

-
- ¹ For an early summary, see Y. Iye in *Physical Properties of High Temperature Superconductors III*, page 285 (1992) Ed. D. M. Ginsburg.
- ² M. Gurvitch and A. T. Fiory Phys. Rev. Lett. **59**, 1337 (1987).
- ³ D. A. Bonn, Ruixing Liang, T. M. Riseman, D. J. Baar, D. C. Morgan, Kuan Zhang, P. Dosanjh, T. L. Duty, A. MacFarlane, G. D. Morris, J. H. Brewer, W. N. Hardy, C. Kallin and A. J. Berlinsky, Phys. Rev. B **47**, 11314 (1993).
- ⁴ T. R. Chien, Z. Z. Wang, and N. P. Ong, Phys. Rev. Lett. **67**, 2088 (1991).
- ⁵ P. W. Anderson, Phys. Rev. Lett. **67**, 2092 (1991).
- ⁶ S. G. Kaplan, S. Wu, H.-T. S. Lihn, H. D. Drew, Q. Li, D. B. Fenner, Julia M. Phillips and S. Y. Hou, Phys. Rev. Lett. **76**, 696 (1996).
- ⁷ J. M. Harris, Y. F. Yan, P. Matl, N. P. Ong, P. W. Anderson, T. Kimura, and K. Kitazawa, Phys. Rev. Lett. **75**, 1391 (1995).
- ⁸ P. Coleman, A. J. Schofield and A. M. Tsvelik, Phys. Rev. Lett. **76**, 1324 (1996).
- ⁹ G. Kotliar, A. Sengupta and C. M. Varma Phys. Rev. B **53**, 3573-3577 (1996).
- ¹⁰ D. K. K. Lee and P. A. Lee, J. Phys.:condens. matt., **9**, 10421, 1997.
- ¹¹ J. Cerne, M. Grayson, D. C. Schmadel, G. S. Jenkins, H. D. Drew, R. Hughes, J. S. Preston, and P. -J. Kung, Phys. Rev. Lett. **84**, 3418 (2000).
- ¹² A. Carrington, A. P. MacKenzie, C. T. Lin, and J. R. Cooper, Phys. Rev. Lett. **69**, 2855 (1992).
- ¹³ B. Stojkovic and D. Pines, Phys. Rev. Lett. **76**, 811 (1996).
- ¹⁴ A. T. Zheleznyak, V. M. Yakovenko, and H. D. Drew, Phys. Rev. B **57**, 3089 (1998).
- ¹⁵ A. T. Zheleznyak, V. M. Yakovenko, and H. D. Drew, Phys. Rev. B **59**, 207 (1999).
- ¹⁶ R. Hlubina and T. M. Rice, Phys. Rev. B **51**, 9253 (1995).
- ¹⁷ L. B. Ioffe and A. J. Millis, Phys. Rev. B **58**, 11631 (1998).
- ¹⁸ D. van der Marel, Phys. Rev. B **60**, R765 (1999).
- ¹⁹ T. Xiang and W.N. Hardy, *unpublished*: cond-mat/0001443.
- ²⁰ Hyekyung Won and Kazumi Maki, Phys. Rev. B **49**, 1397 (1994).
- ²¹ A. Rosch, *unpublished*: cond-mat/9910432.
- ²² O. Narikiyo, *unpublished*: cond-mat/0006028.
- ²³ H. Kontani, K. Kanki and K. Ueda, Phys. Rev. B **59**, 14723 (1999).
- ²⁴ A. J. Millis and A. J. Schofield, *to be published*.
- ²⁵ N. E. Hussey, J. R. Cooper, J. M. Wheatley, I. R. Fisher, A. Carrington, A. P. MacKenzie, C. T. Lin, and O. Milat, Phys. Rev. Lett. **76**, 122 (1996).
- ²⁶ A. Rosch, *private communication*.
- ²⁷ T. Xiang and J. M. Wheatley, Phys. Rev. Lett. **76**, 4632 (1996).
- ²⁸ O. K. Andersen, O. Jepsen, A. I. Liechtenstein and I. I. Mazin, Phys. Rev. B **49**, 4145 (1994).
- ²⁹ A. I. Liechtenstein, O. Gunnarson, O. K. Andersen and R. M. Martin, Phys. Rev. B **54**, 12505 (1996).
- ³⁰ T. Xiang, C. Panagopoulos and J. R. Cooper, International J. Mod. Phys. B **12**, 1007 (1998).
- ³¹ A. Drăgulescu, V. M. Yakovenko and D. J. Singh, Phys. Rev. B **60**, 6312 (1999).
- ³² *Fundamentals of the theory of metals*, A. A. Abrikosov, Elsevier Science Publishers B.V. (1988).
- ³³ A. W. Tyler, Yoichi Ando, F. F. Balakirev, A. Passner, G. S. Boebinger, A. J. Schofield, A. P. Mackenzie and O. Laborde, Phys. Rev. B **57**, R728 (1998).
- ³⁴ Perez Moses and Ross H. McKenzie, Phys. Rev. B **60**, 7998 (1999).
- ³⁵ A. J. Schofield and J. R. Cooper, *to be published*. See cond-mat/9709167 for an earlier preprint.
- ³⁶ R. Hlubina, Phys. Rev. B **58**, 8240 (1998)
- ³⁷ S. D. Obertelli, J. R. Cooper and J. L. Tallon, Phys. Rev. B, **46**, 14928 (1992).
- ³⁸ A. Tyler, PhD Thesis, University of Cambridge, (1998).